ditions, the overall solution error may not be minimal. This is a disadvantage of the method and is due to the fact that the functional is only made stationary and is not minimized.

Acknowledgment

The authors wish to thank D. J. Richards for discussions regarding programming techniques and for obtaining the results presented in Fig. 2.

References

[1] A. Wexler, "Computation of electromagnetic fields," *IEEE Trans. Microwave Theory Tech.*, vol. MTT-17, pp. 416–439, Aug. 1969.
[2] P. C. Dunne, "Complete polynomial displacement fields for finite element method," *J. Roy. Aeronaut. Soc.*, vol. 72, p. 245, 1969.
[3] D. T. Thomas, "Functional approximations for solving boundary value problems by computer," *IEEE Trans. Microwave Theory Tech.*, vol. MTT-17, pp. 447–454, Aug. 1969.
[4] R. M. Bulley, "Analysis of the arbitrarily shaped waveguide by polynomial approximation," *IEEE Trans. Microwave Theory Tech.*, vol. MTT-18, pp. 1022–1028, Dec. 1970.
[5] F. B. Hildebrand, *Methods of Applied Mathematics*, 2nd ed. Englewood Cliffs, N. J.: Prentice-Hall, 1965, p. 219.
[6] P. M. Morse and H. Feshbach, *Methods of Theoretical Physics*, Pt. II. New York: McGraw-Hill, 1953, pp. 1131–1132.
[7] W. J. English, "Vector variational solutions of inhomogeneously loaded cylindrical waveguide structures," *IEEE Trans. Microwave Theory Tech.*, vol. MTT-19, pp. 9–18, Jan. 1971.
[8] L. Fox, *An Introduction to Numerical Linear Algebra.* London, England: Oxford Univ. Press, 1964, pp. 141–142.
[9] D. J. Richards and A. Wexler, "Finite element solutions within curved boundaries," to be published in *IEEE Trans. Microwave Theory Tech.*
[10] S. G. Mikhlin, *Variational Methods in Mathematical Physics.* New York: Macmillan, 1964.

An Analysis of Gap in Microstrip Transmission Lines

MINORU MAEDA, MEMBER, IEEE

Abstract—**Although microstrip transmission lines have been widely used in microwave integrated circuits, the discontinuity structures in the microstrip transmission lines such as a gap, an abruptly ended strip conductor, and so on, have hardly been analyzed. An analytical method and numerical results for a gap capacitance in the microstrip transmission line are described. The equivalent circuit parameters are formulated with three-dimensional Green's functions, based on a variational principle. The numerical results are in good agreement with the published experimental data. The fringing effect of an abruptly ended strip conductor is also investigated.**

I. Introduction

WITH THE RECENT development of microwave integrated circuits, microstrip transmission lines have been widely used as fundamental structures. Since the microwave integrated circuits are fabricated through many processes, such as vacuum deposition, sputtering, electroplating, photoetching, and so on, it is primarily important to design the circuit precisely.

Although a great deal of work has been published on the properties of the microstrip transmission lines [1]–[5], the theoretical and/or experimental results obtained thus far have been almost entirely limited to the characteristic impedance and the phase velocity. Practical microwave integrated circuits, however, have been constructed using a variety of discontinuity structures in the strip conductor, such as a gap, an abruptly ended strip conductor, a tee junction, and so on. Since the discontinuity structures have not been investigated yet, there appears to be a need for rigorous theoretical formulas on the discontinuity structures.

This paper describes an analytical method and numerical results for a gap capacitance in the strip conductor of the microstrip transmission line. The gap capacitance of the symmetric-strip transmission line has been investigated theoretically and experimentally by Altschuler and Oliner [6]. For the gap capacitance of the microstrip transmission line, however, only experimental results obtained by Stinehelfer have been published [7]. The analytical method presented here employs a variational principle for formulating the problems based on an electrostatic approximation, and derives the theoretical expressions for the equivalent circuit parameters using three-dimensional potential Green's functions. The numerical results, obtained with the aid of a digital computer, are compared with the published experimental data. The derived formulas can be applied to investigate the fringing effect of the abruptly ended strip conductor when the gap is of in-

Manuscript received July 12, 1971; revised September 7, 1971.
The author is with Central Research Laboratory, Hitachi, Ltd., Kokubunji, Tokyo, Japan.

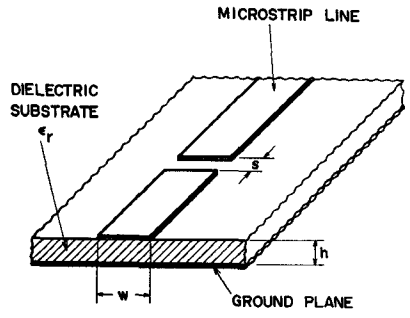

Fig. 1. Physical structure of gap in microstrip transmission line.

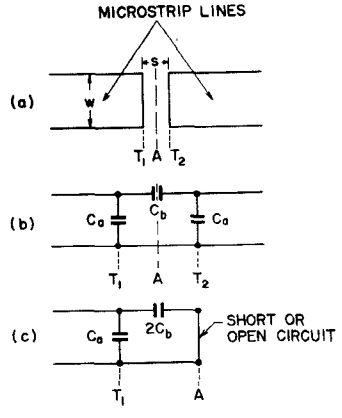

Fig. 2. Gap in microstrip transmission line. (a) Physical structure. (b) Equivalent circuit. (c) Equivalent circuit for analysis.

finite spacing. The fringing capacitances are also calculated [8] and compared with the experimental data of Napoli and Hughes [9].

II. Equivalent Circuit Parameters of Gap Structure

The physical gap structure in the strip conductor of the microstrip transmission line is shown in Fig. 1. The arbitrary discontinuity at a junction of two transmission lines can be generally represented by either the equivalent tee or pi circuit [10]. It is preferable to represent the gap structure with the equivalent pi circuit as shown in Fig. 2, because the parameters of the equivalent pi circuit show the physical meanings well. The shunt-gap capacitance C_a can be inferred from the effect of the disorder of the electrostatic field distribution at the edge of the strip conductor. The series capacitance C_b arises from the coupling effect of the adjacent strip conductors. The terminal plane T of the equivalent circuit in Fig. 2 is chosen at the edge of the strip conductor.

Let the electric wall or the magnetic wall be placed along the center line as shown in Fig. 2(a). This corresponds to the equivalent circuit with a short circuit or an open circuit in the symmetrical plane. Hence, the equivalent-circuit parameters C_e and C_m for the new equivalent circuit shown in Fig. 2(c) are given by

$$C_e = C_a + 2C_b \tag{1}$$

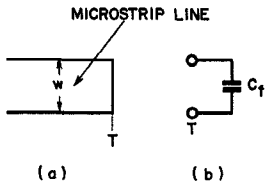

Fig. 3. Abruptly ended strip conductor in microstrip transmission line. (a) Physical structure. (b) Equivalent circuit.

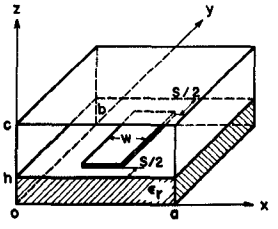

Fig. 4. Analytical configuration of gap in microstrip transmission line.

$$C_m = C_a \tag{2}$$

where the subscripts e and m correspond to the electric and magnetic walls, respectively.

The abruptly ended strip conductor can be represented by the equivalent circuit as shown in Fig. 3. The fringing capacitance C_f, which arises from the disorder of the electrostatic field at the edge of the strip conductor, can be obtained when the gap is of infinite spacing.

The analytical configuration of the gap is illustrated in Fig. 4. If the electric walls or the magnetic walls are placed at $y=0$ and $y=b$, the total capacitance C_{ti} is given by

$$C_{ti} = C_0 + 2C_i, \qquad i = e, m \tag{3}$$

where C_0 is the line capacitance of the uniform microstrip transmission line with its length of $b-s$. Let the three-dimensional potential Green's function, satisfying the boundary conditions with the electric walls ($i=e$) or the magnetic walls ($i=m$) at $y=0$, and b be $G_i(x, y, z|x', y', z')$, and the charge distribution on the strip conductor be $\rho_i(x, y, z)$. Then the capacitance C_{ti} is given by the variational expression which is stationary with respect to arbitrary first-order variations in the charge distribution $\rho_i(x, y, z)$ [11]:

$$\frac{1}{C_{ti}} = \frac{\int\int \rho_i(x, y, z) G_i(x, y, z, |x', y', z') \rho_i(x', y', z')\, dv dv'}{\left[\int \rho_i(x, y, z)\, dv\right]^2} \tag{4}$$

where the integral is to be taken through all the volume in which the charge is distributed. Since this is a "lower bound" type of variational expression, the capacitance can be obtained by maximizing, with a suitable choice of the charge distribution as a trial function.

III. Derivation of Green's Function

The three-dimensional potential Green's function is the solution of the following Poisson's equation:

$$\nabla^2 G_i(x, y, z|x', y', z') = -\frac{1}{\epsilon}\delta(x-x')\delta(y-y')\delta(z-z') \quad (5)$$

where $\delta(x-x')$ is a Dirac's delta function. If it is assumed that the strip conductor is infinitely thin, the Green's functions for the case $z=h$ are adequate for the calculation of the capacitance C_{ti} using the variational expression (4). Of course, the Green's functions should satisfy the required boundary and continuity conditions.

The Green's function $G_e(x, y, z|x', y', h)$ for the electric walls should satisfy the following conditions:

$$G_e(0, y, z|x', y', h) = 0 \quad (6a)$$
$$G_e(a, y, z|x', y', h) = 0 \quad (6b)$$
$$G_e(x, 0, z|x', y', h) = 0 \quad (6c)$$
$$G_e(x, b, z|x', y', h) = 0 \quad (6d)$$
$$G_e(x, y, 0|x', y', h) = 0 \quad (6e)$$
$$G_e(x, y, c|x', y', h) = 0 \quad (6f)$$
$$G_e(x, y, h-0|x', y', h) = G_e(x, y, h+0|x', y', h) \quad (6g)$$
$$\frac{\partial}{\partial x}G_e(x, y, h-0|x', y', h) = \frac{\partial}{\partial x}G_e(x, y, h+0|x', y', h) \quad (6h)$$
$$\frac{\partial}{\partial y}G_e(x, y, h-0|x', y', h) = \frac{\partial}{\partial y}G_e(x, y, h+0|x', y', h). \quad (6i)$$

The Poisson's equation (5) can be readily solved as a linear combination of hyperbolic sinusoidal functions. By applying the above boundary conditions to the solution, $G_e(x, y, z|x', y', h)$ is found to be

$$G_e(x, y, z|x', y', h) = \begin{cases} \sum_{m=1}^{\infty}\sum_{n=1}^{\infty} \frac{4}{ab\gamma_{mn}\Gamma_{mn}} \sin\left(\frac{m\pi x}{a}\right)\sin\left(\frac{m\pi x'}{a}\right) \\ \cdot\sin\left(\frac{n\pi y}{b}\right)\sin\left(\frac{n\pi y'}{b}\right)\sinh(\gamma_{mn}z) \\ \cdot\sinh(\gamma_{mn}(c-h)), \quad 0 \leqq z \leqq h \\ \sum_{m=1}^{\infty}\sum_{n=1}^{\infty} \frac{4}{ab\gamma_{mn}\Gamma_{mn}} \sin\left(\frac{m\pi x}{a}\right)\sin\left(\frac{m\pi x'}{a}\right) \\ \cdot\sin\left(\frac{n\pi y}{b}\right)\sin\left(\frac{n\pi y'}{b}\right)\sinh(\gamma_{mn}(c-z)) \\ \cdot\sinh(\gamma_{mn}h), \quad h \leqq z \leqq c \end{cases} \quad (7)$$

where

$$\gamma_{mn} = \sqrt{\left(\frac{m\pi}{a}\right)^2 + \left(\frac{n\pi}{b}\right)^2} \quad (8)$$

$$\Gamma_{mn} = \epsilon_r \cosh(\gamma_{mn}h)\sinh(\gamma_{mn}(c-h)) + \sinh(\gamma_{mn}h)\cosh(\gamma_{mn}(c-h)). \quad (9)$$

On the other hand, the Green's function $G_m(x, y, z|x', y', h)$ for the magnetic walls should satisfy the following boundary conditions at $y=0$ and $y=b$:

$$\frac{\partial}{\partial y}G_m(x, 0, z|x', y', h) = 0 \quad (10a)$$
$$\frac{\partial}{\partial y}G_m(x, b, z|x', y', h) = 0. \quad (10b)$$

The other boundary and continuity conditions are the same as the case of the Green's function $G_e(x, y, z|x', y', h)$. Through similar mathematical manipulations, $G_m(x, y, z|x', y', h)$ can be derived as follows:

$$G_m(x, y, z|x', y', h) = \begin{cases} \sum_{m=1}^{\infty}\sum_{n=0}^{\infty} \frac{4\sigma_n}{ab\gamma_{mn}\Gamma_{mn}} \sin\left(\frac{m\pi x}{a}\right)\sin\left(\frac{m\pi x'}{a}\right) \\ \cdot\cos\left(\frac{n\pi y}{b}\right)\cos\left(\frac{n\pi y'}{b}\right)\sinh(\gamma_{mn}z) \\ \cdot\sinh(\gamma_{mn}(c-h)), \quad 0 \leqq z \leqq h \\ \sum_{m=1}^{\infty}\sum_{n=0}^{\infty} \frac{4\sigma_n}{ab\gamma_{mn}\Gamma_{mn}} \sin\left(\frac{m\pi x}{a}\right)\sin\left(\frac{m\pi x'}{a}\right) \\ \cdot\cos\left(\frac{n\pi y}{b}\right)\cos\left(\frac{n\pi y'}{b}\right)\sinh(\gamma_{mn}(c-z)) \\ \cdot\sinh(\gamma_{mn}h), \quad h \leqq z \leqq c \end{cases} \quad (11)$$

where

$$\sigma_n = \begin{cases} \frac{1}{2}, & n = 0 \\ 1, & n \neq 0. \end{cases}$$

The term for $n=0$ in (11) can be written as

$$\begin{cases} \sum_{m=1}^{\infty} \frac{1}{b}\frac{2}{m\pi\Gamma_{m0}} \sin\left(\frac{m\pi x}{a}\right)\sin\left(\frac{m\pi x'}{a}\right)\sinh\left(\frac{m\pi z}{a}\right) \\ \cdot\sinh\left(\frac{m\pi(c-h)}{a}\right), \quad 0 \leqq z \leqq h \\ \sum_{m=1}^{\infty} \frac{1}{b}\frac{2}{m\pi\Gamma_{m0}} \sin\left(\frac{m\pi x}{a}\right)\sin\left(\frac{m\pi x'}{a}\right)\sinh\left(\frac{m\pi(c-z)}{a}\right) \\ \cdot\sinh\left(\frac{m\pi h}{a}\right), \quad h \leqq z \leqq c. \end{cases} \quad (12)$$

It should be noted that the term, except for the coefficient $1/b$, corresponds to the two-dimensional Green's function in the rectangular boundary for the cross section of the uniform microstrip transmission line obtained by Yamashita [12]. This fact indicates that the capacitance calculated with (12) is the line capacitance of the uniform microstrip transmission line with its length of b.

IV. Formulation of Equivalent Circuit Parameters

For the infinitely thin strip-conductor case, the charge distribution may take the form

$$\rho_i(x, y, z) = \rho_i'(x, y)\delta(z-h). \quad (13)$$

Then (4) becomes

$$\frac{1}{C_{ti}} = \frac{\iint \rho_i'(x, y) G_i(x, y, h \mid x', y', h) \rho_i'(x', y')\, ds ds'}{\left[\int \rho_i(x, y)\, ds\right]^2} \cdot \quad (14)$$

As a charge distribution on an infinitely thin strip conductor of the uniform microstrip transmission line, the following expression has been used by Yamashita [13] and found to give sufficiently accurate results on the characteristic impedance and the phase velocity:

$$f(x) = 1 + \left|\frac{2}{w}\left(x - \frac{a}{2}\right)\right|^3, \qquad \left|x - \frac{a}{2}\right| \leqq \frac{w}{2} \cdot \quad (15)$$

It is reasonable to consider that the charge density in the longitudinal direction also increases near the edge of the strip conductor. Hence the following form of the charge distribution is assumed in this paper:

$$\rho_i'(x, y) = f(x) g(y) \quad (16)$$

and

$$g(y) = \begin{cases} 0, & \dfrac{b}{2} - \dfrac{s}{2} \leqq \left|y - \dfrac{b}{2}\right| \leqq \dfrac{b}{2} \\ 1 + \dfrac{K}{h}\left(\left|y - \dfrac{b}{2}\right| - \dfrac{b}{2} + \dfrac{s}{2} + h\right), & \dfrac{b}{2} - \dfrac{s}{2} - h \leqq \left|y - \dfrac{b}{2}\right| \leqq \dfrac{b}{2} - \dfrac{s}{2} \\ 1, & \left|y - \dfrac{b}{2}\right| \leqq \dfrac{b}{2} - \dfrac{s}{2} - h \end{cases} \quad (17)$$

where the shield walls are assumed to be sufficiently apart from the strip conductor. The coefficient K is to be determined so as to maximize the capacitance C_{ti}.

The capacitances C_{te}, C_{tm}, and C_0 can be obtained by substituting (7), (11), (12), (15), and (17) into (14) as follows:

$$C_{te} = \frac{\frac{25}{16} b \left(1 - \frac{s}{b} + K \frac{h}{b}\right)^2}{\sum_{m=1,3,\cdots}^{\infty} \sum_{n=1,3,\cdots}^{\infty} \frac{4 P_m^2 R_n^2}{a \gamma_{mn} \Gamma_{mn}} \left(\frac{s}{b}\right)^2 \sinh(\gamma_{mn} h) \sinh(\gamma_{mn}(c - h))} \quad (18)$$

$$C_{tm} = \frac{\frac{25}{16} b \left(1 - \frac{s}{b} + K \frac{h}{b}\right)^2}{\sum_{m=1,3,\cdots}^{\infty} \frac{2 P_m^2}{m\pi \Gamma_{m0}} \left(1 - \frac{s}{b} + K \frac{h}{b}\right)^2 \sinh\left(\frac{m\pi h}{a}\right) \sinh\left(\frac{m\pi(c - h)}{a}\right) + \sum_{m=1,3,\cdots}^{\infty} \sum_{n=2,4,\cdots}^{\infty} \frac{4 P_m^2 Q_n^2}{a \gamma_{mn} \Gamma_{mn}} \left(\frac{s}{b}\right)^2 \sinh(\gamma_{mn} h) \sinh(\gamma_{mn}(c - h))} \quad (19)$$

$$C_0 = \frac{\frac{25}{16}(b - s)}{\sum_{n=1,3,\cdots}^{\infty} \frac{2 P_m^2}{m\pi \Gamma_{m0}} \sinh\left(\frac{m\pi h}{a}\right) \sinh\left(\frac{m\pi(c-h)}{a}\right)} \quad (20)$$

where

$$P_m = 2\left(\frac{2a}{m\pi w}\right) \sin\left(\frac{m\pi w}{2a}\right) + 3\left(\frac{2a}{m\pi w}\right)^2 \cos\left(\frac{m\pi w}{2a}\right) - 6\left(\frac{2a}{m\pi w}\right)^3 \sin\left(\frac{m\pi w}{2a}\right) - 6\left(\frac{2a}{m\pi w}\right)^4 \cdot \cos\left(\frac{m\pi w}{2a}\right) - 6\left(\frac{2a}{m\pi w}\right)^4 \quad (21)$$

$$Q_n = \left(\frac{2b}{n\pi s}\right) \cos\left(\frac{n\pi s}{2b}\right) + K\left[\left(\frac{2b}{n\pi s}\right) \sin\left(\frac{n\pi s}{2b}\right) - \left(\frac{2b}{n\pi s}\right)\left(\frac{2b}{n\pi h}\right) \sin\left(\frac{n\pi s}{2b} + \frac{n\pi h}{2b}\right) \cdot \sin\left(\frac{n\pi h}{2b}\right)\right] \quad (22)$$

$$R_n = \left(\frac{2b}{n\pi s}\right) \cos\left(\frac{n\pi s}{2b}\right) + K\left[\left(\frac{2b}{n\pi s}\right) \cos\left(\frac{n\pi s}{2b}\right) - \left(\frac{2b}{n\pi s}\right)\left(\frac{2b}{n\pi h}\right) \cos\left(\frac{n\pi s}{2b} + \frac{n\pi h}{2b}\right) \cdot \sin\left(\frac{n\pi h}{2b}\right)\right]. \quad (23)$$

Numerical data for the equivalent circuit parameters of the gap can be readily obtained by computing the above formulas with the aid of a digital computer and using (1)-(3).

V. Numerical Results

The formulas derived above are for the gap in the shielded microstrip transmission line in the strict sense. However, when the shield walls in Fig. 4 are sufficiently removed from the strip conductor, the structure approaches the microstrip case. The numerical computations were carried out in this paper for the case where the effects of the shield walls are negligible.

The values of the gap capacitances C_a and C_b for 50-Ω microstrip transmission lines with the dielectric thickness of 0.5 mm are plotted as a function of s/h in Fig. 5. The series capacitance C_b decreases as the gap spacing increases. This tendency has been expected because the

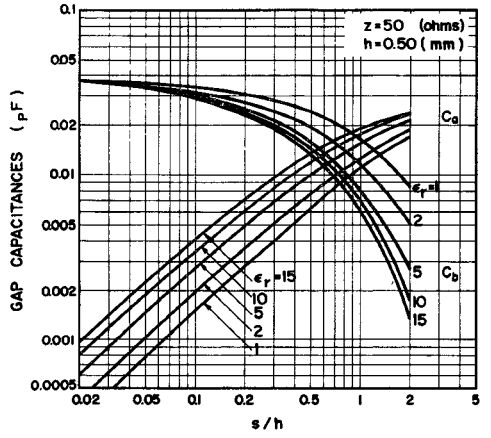

Fig. 5. Gap capacitances for 50-Ω microstrip transmission line as a function of s/h ($h=0.50$ mm).

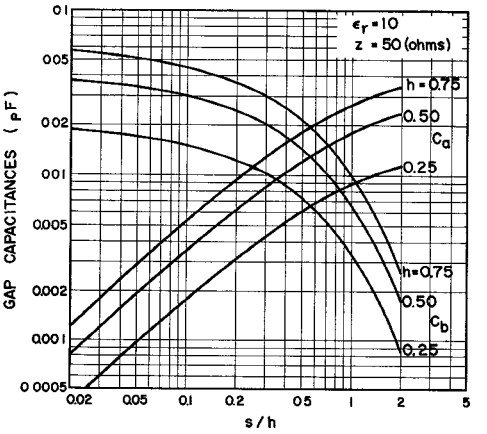

Fig. 6. Gap capacitances for 50-Ω microstrip transmission line as a function of s/h ($\epsilon_r=10$).

TABLE I
OPTIMUM COEFFICIENT OF CHARGE DISTRIBUTION

	K_e							K_m							
ϵ_r / S/h	1	2	3	5	7	10	15	1	2	3	4	5	7	10	15
0.02	2	2	2	2	2	2	2	0	0	0	0	0	0	0	0
0.04	2	2	2	2	2	2	2	0	0	0	0	0	0	0	0
0.06	2	2	2	2	2	2	2	0	0	0	0	0	0	0	0
0.1	2	2	2	2	2	2	1	0	0	0	0	0	0	0	0
0.2	2	2	2	2	2	1	1	0	0	0	0	0	0	0	0
0.4	2	2	2	1	1	1	1	0	0	0	0	0	0	0	0
0.6	2	2	1	1	1	1	1	1	0	0	0	0	0	0	0
1.0	2	1	1	1	1	1	1	1	1	1	1	1	1	1	1
2.0	2	1	1	1	1	1	1	1	1	1	1	1	1	1	1

Note: $Z=50$ Ω; $h=0.50$ mm.

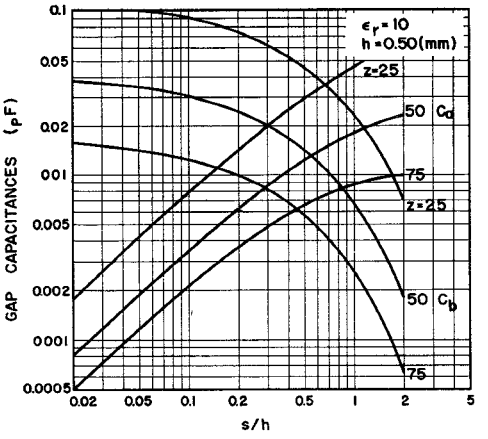

Fig. 7. Gap capacitances for microstrip transmission line as a function of s/h ($\epsilon_r=10$, $h=0.50$ mm).

electrostatic coupling between two conductors becomes loose when the conductors keep apart from each other. When the ratio s/h is sufficiently large, C_b becomes negligible and the structure approaches the simple abruptly ended strip conductor.

The numerical calculations were carried out by the digital computer HITAC 5020 F. The summation of the infinite series was truncated when the last term added was less than one 10^8th of the first term. The calculation time of C_a and C_b was about 200 s/structure, although it depended on the dimensions of a gap structure. Of course, the coefficient K of the charge distribution $g(y)$ was chosen so as to maximize the variational expression. In order to reduce the computation time, integers were employed for K. Optimum coefficients for the electric and magnetic walls are tabulated in Table I. It can be seen from Table I that the charge distributions for the electric and magnetic walls take the same shape when the gap spacing becomes large, and that we may set K equal to unity for calculating the fringing capacitance of the abruptly ended strip conductor.

The calculated gap capacitances for various structures are shown in Figs. 6 and 7. Fig. 8 shows the normalized strip width w/h as a function of relative dielectric constant ϵ_r for typical values of characteristic impedance.

Since the numerical data for the fringing capacitance of the abruptly ended strip conductor are useful for the designs of filters, open stubs, and so on, the calculated results for various parameters are shown in Fig. 9. The computation time C_f was about 40 s/structure, because the coefficient K was set equal to unity beforehand.

The present theory was compared with the experimental data of Stinehelfer for the series gap capacitance C_b, with $\epsilon_r=8.875$, $h=0.508$ mm, and $w=0.508$ mm. The calculated gap capacitances for the parameters are shown along with the experimental ones in Fig. 10. It is seen in the figure that the calculated values are in fairly good agreement with the measured values. The fringing capacitance of the abruptly ended strip con-

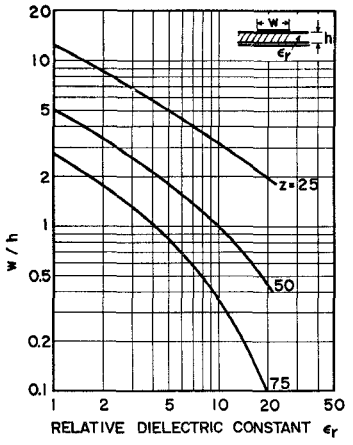

Fig. 8. Normalized strip width as a function of relative dielectric constant ϵ_r.

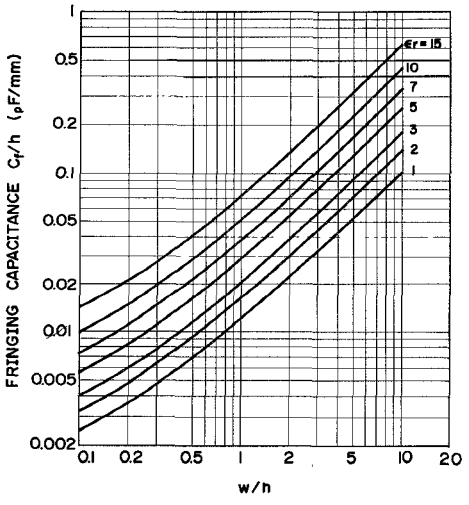

Fig. 9. Fringing capacitance for microstrip transmission line as a function of w/h.

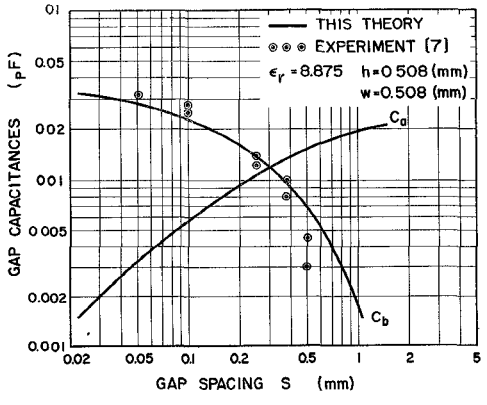

Fig. 10. Theoretical and experimental gap capacitances for microstrip transmission line.

ductor calculated by this theory was compared with the one experimentally obtained by Napoli and Hughes. Since the experimental data have been obtained in terms of an effective increase in line length, the calculated fringing capacitance was transformed into the same expression, based on the following equation:

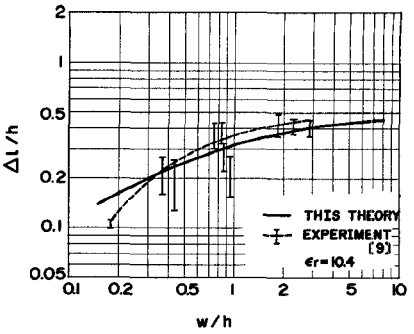

Fig. 11. Comparison of this theory with measured fringing effect of abruptly ended strip conductor.

$$\frac{\Delta l}{h} = C_f \frac{Z_0 v}{h} \tag{24}$$

where Z_0 is a characteristic impedance and v a phase velocity. Fig. 11 compares the calculated and measured fringing effect, and shows a good fit.

VI. Conclusion

In this paper the gap in the strip conductor of the microstrip transmission line is analyzed by the application of a variational principle. The equivalent circuit parameters of the gap are formulated using potential Green's functions and approximate charge distributions. The theoretical formulas can be applied to the fringing effect of the abruptly ended strip conductor when the gap is of infinite spacing. Numerical calculations are carried out with the aid of a digital computer. The theoretical results are compared with the published experimental data, and are shown to give accurate results.

Acknowledgment

The author wishes to thank his colleagues for many helpful discussions.

References

[1] H. A. Wheeler, "Transmission-line properties of parallel strips separated by a dielectric sheet," *IEEE Trans. Microwave Theory Tech.*, vol. MTT-13, pp. 172–175, Mar. 1965.
[2] H. E. Stinehelfer, Sr., "An accurate calculation of uniform microstrip transmission lines," *IEEE Trans. Microwave Theory Tech.*, vol. MTT-16, pp. 439–444, July 1968.
[3] E. Yamashita and R. Mittra, "Variational method for the analysis of microstrip lines," *IEEE Trans. Microwave Theory Tech.*, vol. MTT-16, pp. 251–256, Apr. 1968.
[4] T. G. Bryant and J. A. Weiss, "Parameters of microstrip transmission lines and of coupled pairs of microstrip lines," *IEEE Trans. Microwave Theory Tech.*, vol. MTT-16, pp. 1021–1027, Dec. 1968.
[5] P. Silvester, "TEM wave properties of microstrip transmission lines," *Proc. Inst. Elec. Eng. (London)*, vol. 115, pp. 43–48, Jan. 1968.
[6] H. M. Altschuler and A. A. Oliner, "Discontinuity in the center conductor of symmetric strip transmission line," *IRE Trans. Microwave Theory Tech.*, vol. MTT-8, pp. 328–339, May 1960.
[7] The Microwave Engineers' Handbook and Buyers' Guide.

New York: Horizon House, Feb. 1969, p. 72.
[8] A. Farrar and A. T. Adams, "Computation of lumped microstrip capacities by matrix methods—Rectangular sections and end effect," *IEEE Trans. Microwave Theory Tech.* (Corresp.), vol. MTT-19, pp. 495–497, May 1971.
[9] L. S. Napoli and J. J. Hughes, "Foreshortening of microstrip open circuits on alumina substrates," *IEEE Trans. Microwave Theory Tech.* (Corresp.), vol. MTT-19, pp. 559–561, June 1971.
[10] N. Marcuvitz, *Waveguide Handbook*. New York: McGraw-Hill, 1951, p. 108.
[11] R. E. Collin, *Field Theory of Guided Waves*. New York: McGraw-Hill, 1960, p. 148.
[12] E. Yamashita and K. Atsuki, "Strip line with rectangular outer conductor and three dielectric layers," *IEEE Trans. Microwave Theory Tech.*, vol. MTT-18, pp. 238–244, May 1970.
[13] E. Yamashita, "Variational method for the analysis of microstrip-like transmission lines," *IEEE Trans. Microwave Theory Tech.*, vol. MTT-16, pp. 529–535, Aug. 1968.

A Proposed Lumped-Element Switching Circulator Principle

REINHARD H. KNERR, MEMBER, IEEE

Abstract—**Two different analytical methods, the complex conjugate input admittance approach and the eigenvalue analysis, show the possibility of building a fast switching lumped-element circulator. In conventional switching circulators, switching is achieved by changing the required magnetic biasing field. The proposed principle, which is valid for circulators of all types, is especially interesting for lumped-element circulators where the switching may be accomplished by simply changing two capacitor values. The capacitors could be switched by varying voltages on semiconductors thus permitting very fast switching. The analysis has been experimentally verified. No attempt to obtain optimization of a specific design was made.**

Introduction

In the course of efforts to develop a high-performance photo-processed lumped-element circulator and appropriate analysis [1]–[3], it was discovered that it should be possible to switch the sense of circulation by switching parameters other than the magnetic biasing field. While this observation is valid in principle for circulators of all types, it is especially interesting for lumped-element circulators where the switching may be accomplished simply by changing lumped capacitors. In principle the capacitors could be switched by varying voltages on semiconductors, thus permitting very fast switching. The possibility of such a switching circulator was treated in passing in [2] and [3]. This paper will expand upon the analysis of the device.

In 1965 Konishi [4] and Dunn and Roberts [5] published papers describing lumped-element circulators at the heart of which were three inductors coupled through a common ferrite disk and resonated by individual capacitors. Various approaches have been taken to analyze this basic circulator type [1]–[8]. The author involves [1] an extension of Deutsch and Wieser's method [7] that will be referred to as the complex input-admittance method. The analysis of the more complex structures studied by the author is reported in [2] and [3]. This is an eigenvalue analysis that has been found extremely valuable in providing a fundamental understanding of the circulator operation and near quantitative performance predictions.

In this paper, each of these approaches will be used to demonstrate the principle of capacitive switching. References [2] and [3] will be relied upon for details of the eigenvalue analysis. Since [1] does not give any details of the complex input-admittance analysis, it will be outlined in this paper.

I. The Complex Input-Admittance Analysis

There is a well-known theorem [9] that states: a lossless three-port can only be matched at all three ports if it contains a lossless nonreciprocal element, and such a matched three-port represents an ideal circulator.

If the three-port in Fig. 1 is represented by

$$\begin{bmatrix} V_1 \\ V_2 \\ V_3 \end{bmatrix} = \begin{bmatrix} \alpha & \beta & \gamma \\ \gamma & \alpha & \beta \\ \beta & \gamma & \alpha \end{bmatrix} \begin{bmatrix} i_1 \\ i_2 \\ i_3 \end{bmatrix} \tag{1}$$

i.e., $[V] = [Z][i]$, then this three-port is lossless if

$$\text{Re}\,(\alpha) = 0 \quad \text{and} \quad \beta = -\gamma^* \tag{2}$$

where γ^* designates the complex conjugate of γ. It has been shown that the impedance matrix of the three-port

Manuscript received July 14, 1971; revised September 13, 1971.
The author is with Bell Laboratories, Inc., Allentown, Pa. 18103.